JACS
JOURNAL OF THE AMERICAN CHEMICAL SOCIETY
pubs.acs.org/JACS
Communication

DNA-Regulated Multi-Protein Complement Control

Yinglun Ma, Peter H. Winegar, C. Adrian Figg, Namrata Ramani, Alex J. Anderson, Kathleen Ngo, John F. Ahrens, Nikhil S. Chellam, Young Jun Kim, and Chad A. Mirkin*

Cite This: J. Am. Chem. Soc. 2024, 146, 32912−32918
Read Online
ACCESS | Metrics & More | Article Recommendations | Supporting Information

ABSTRACT: In nature, the interactions between proteins and their complements/substrates can dictate complex functions. Herein, we explore how DNA on nucleic acid modified proteins can be used as scaffolds to deliberately control interactions with a peptide complement (by adjusting length, sequence, and rigidity). As model systems, split GFPs were covalently connected through DNA scaffolds (36−58 bp). Increasing the length or decreasing the rigidity of the DNA scaffold (through removal of the duplex) increases the extent of intramolecular protein binding (up to 7.5-fold) between these GFP fragments. Independent and dynamic control over functional outputs can also be regulated by DNA hybridization; a multi-protein (split CFP and YFP) architecture was synthesized and characterized by fluorescence. This ternary construct shows that DNA displacement strands in different stoichiometric ratios can be used deliberately to regulate competitive binding between two unique sets of proteins. These studies establish a foundation for creating new classes of biological machinery based upon the concept of DNA-regulated multi-protein complement control.

Proteins and their complement/substrate interactions regulate functions essential for life, including those that maintain structural integrity and those responsible for molecular transport, light harvesting, luminescence, catalysis, and cellular signaling.[1−6] Current synthetic methods to program these interactions, such as *de novo* design[7−9] and protein engineering,[10−14] have enabled the construction of one-, two-, and three-dimensional protein systems that are responsive to chemical, optical, and enzymatic stimuli.[15−19] However, such methods are often limited either by inaccurate predictions in *de novo* design (e.g., insufficient training data) or loss of function (when engineering new target protein interaction interfaces).[20] Despite these technological advances, it is challenging to design dynamic interactions between proteins and their complements that lead to multiple functional outputs.[21,22] The ability to control the interactions between an increasing number of proteins and their complements not only would enable the manipulation of complex natural functions, but is also necessary to design new classes of biological machinery.

DNA hybridization is a powerful tool to program the assembly of proteins and other nanoscale materials.[23−31] When attached to protein surfaces, DNA can be used to control protein−protein interactions by replacing target protein binding interfaces with specific DNA−DNA interactions, facilitating protein assembly into crystalline, polymeric, and heteroprotein architectures.[32−40] Moreover, DNA can also be used as scaffolds to organize proteins and modulate interactions with their complements, alongside related functions.[41−46] However, the effects of DNA scaffold length and rigidity on protein-complement binding (PCB) remain underexplored, especially in systems containing more than two proteins.[47−53] This understanding is essential to design DNA-addressable multi-component protein systems that exhibit desired functionality.

In this study, we report the design and synthesis of dynamic DNA scaffolds to control spontaneous binding between the split green fluorescent protein (GFP) fragments GFP_{1-10} and FP_{11}.[54,55] In a proof-of-concept experiment, we extend these design variables within this binary model system to a ternary split cyan and yellow fluorescent protein (CFP and YFP) fragment assembly comprising CFP_{1-10}, FP_{11}, and YFP_{1-10},[56,59] where the DNA scaffold enables orthogonal control over unique sets of protein fragment binding events. Taken together, this work uses DNA scaffolds to systematically study the PCB design space for multi-component protein architectures.

Split GFP is an excellent system to study PCB with DNA; its constituent fragments GFP_{1-10} and FP_{11} are nonfluorescent when dissociated, but can spontaneously bind (K_D = 0.5 μM; $\lambda_{ex/em}$ = 488/510 nm), leading to chromophore maturation which results in fluorescence.[54,55,57−60] However, this binding event requires these fragments to be close to one another, taking up to 24 h to achieve maximum fluorescence.[57,59] Thus, we hypothesized that a DNA scaffold can control this binding equilibrium. In this construct, GFP_{1-10} and FP_{11} are attached to individual DNA strands (Scheme 1, **1** and **2**) that can be duplexed for end-to-end separation; this rigid, double-stranded scaffold (**3**) then limits binding between fragments. When the duplexing strand is removed, a flexible, single-stranded scaffold forms that allows the proteins to spontaneously bind (**4**). Duplexing varying lengths of DNA strands can change the scaffold rigidity, thereby impacting the extent to which these

Received: August 16, 2024
Revised: November 14, 2024
Accepted: November 15, 2024
Published: November 21, 2024

https://doi.org/10.1021/jacs.4c11315
J. Am. Chem. Soc. 2024, 146, 32912−32918

Scheme 1. DNA Scaffold Mediated Control Over Protein-Complement Binding for GFP1-10 and FP11

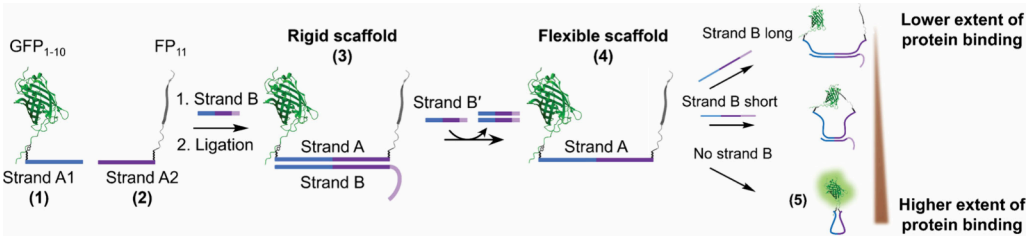

[a]GFP_{1-10}-A1 (**1**) and A2-FP_{11} (**2**) assemble on strand B to scaffold the proteins on a rigid DNA duplex (**3**); strand displacement of strand B with strand B′ results in a flexible single-stranded DNA scaffold (**4**); The extent of protein binding (**5**) can be tuned by varying the length/design of duplexing strand.

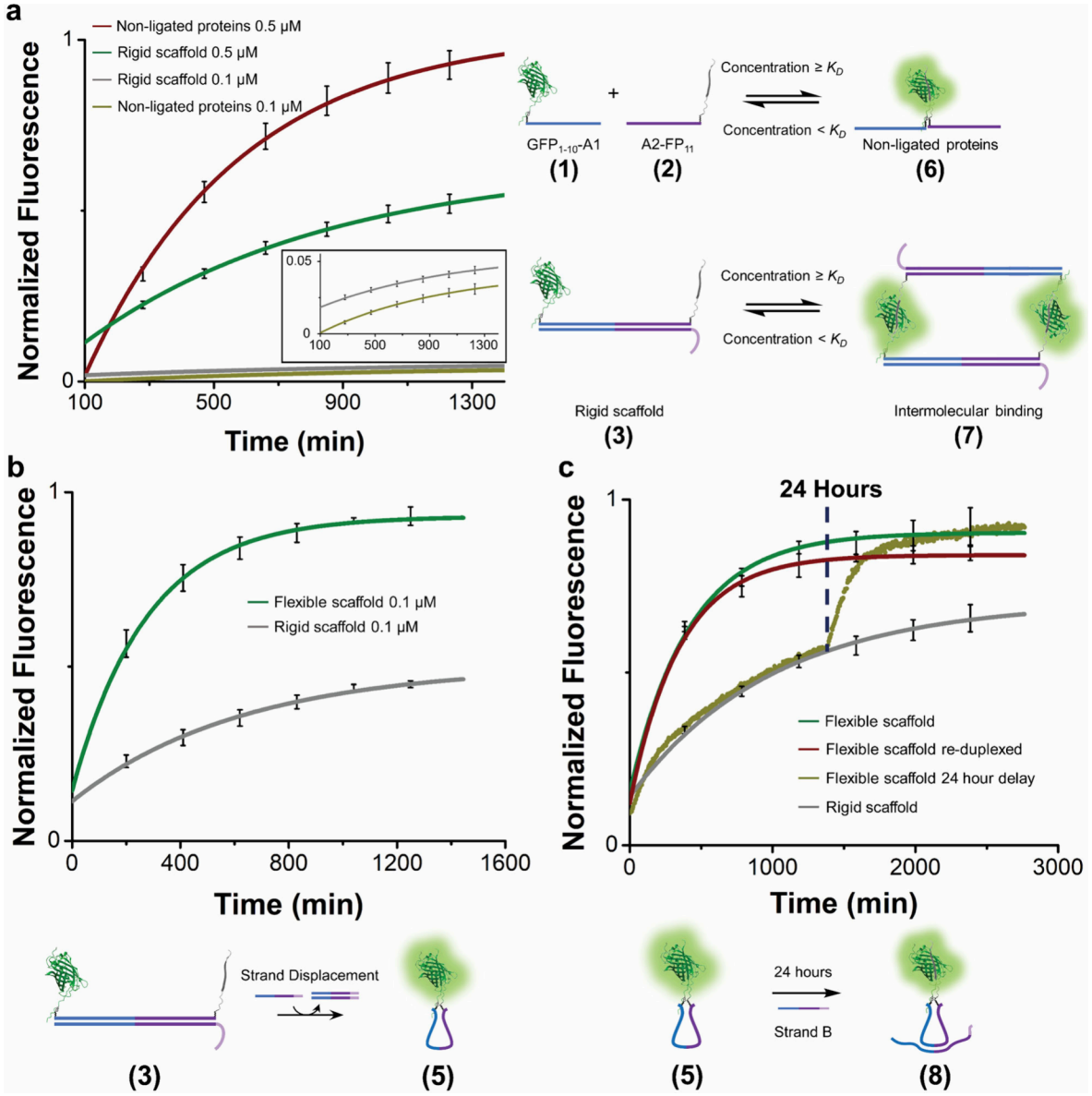

Figure 1. (a) Fluorescence monitoring of protein binding at K_D (0.5 μM) and below K_D (0.1 μM). (b) Removal of strand B from the rigid scaffold results in higher extents of protein binding. (c) Scaffold flexibility can be temporally controlled via DNA interactions; however, bound GFP_{1-10}-FP_{11} could not be separated after reduplexing the scaffold with additional strand B.

fragments can bind to one another. Mutant GFP_{1-10} was modified with a C-terminal oligonucleotide, yielding protein−DNA construct **1** while FP_{11} was modified with an N-terminal oligonucleotide, resulting in construct **2** (Figures S1−S5). This synthetic process yields a covalently linked, unimolecular protein−DNA construct (**3**). Previously reported protein assemblies do not covalently link such DNA strands (e.g., **1** and **2**) as they were initially assembled within binding

https://doi.org/10.1021/jacs.4c11315
J. Am. Chem. Soc. 2024, 146, 32912−32918

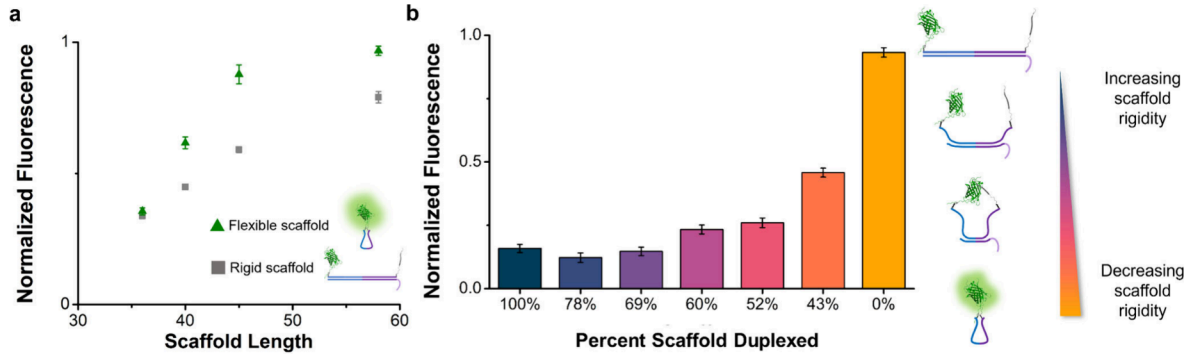

Figure 2. (a) An increasing PCB amount is observed by increasing the scaffold length. The rigid scaffold is indicated by the gray square, while the flexible scaffold is indicated by the green triangle. (b) The percent of the scaffold duplexed dictates the rigidity of the scaffold, which in turn can dictate the extent of intramolecular PCB. All fluorescence measurements were collected after ∼17 h.

proximity via weaker, reversible DNA−DNA interactions.[24,42,51,53,61] However, covalent interactions in the "flexible" DNA scaffold are necessary for binding between scaffolded units (i.e., intramolecular binding; **5**). These covalent interactions allowed **1** and **2** to remain tethered when the "rigid" scaffold was converted to a flexible one. Therefore, the rigid scaffold was assembled with a mixture of **1**, **2**, and strand B followed by ligation (11% ligation yield via SDS-PAGE; Figures S6, S7). Subsequently, strand B′ was added in excess to the rigid scaffold for toehold-mediated strand displacement (TMSD) on strand B, which generated the flexible scaffold **4**. The concentration-dependent fluorescence of the scaffolded proteins was studied to quantify the ratio of intra (**5**)- to intermolecular binding (i.e., binding between protein units on different scaffolds; **7**). We found the K_D for this split GFP system to be 0.5 μM, which is consistent with prior reports (Figures S8, S9, Table S3).[57,59] Thus, the scaffolded proteins were studied at concentrations below K_D (0.1 μM) and at K_D (0.5 μM) to evaluate if intermolecular interactions influenced PCB (Figure 1a).

From these time-dependent fluorescence measurements, the 0.5 μM mixture of **1** and **2** exhibited a ∼ 33× higher maximum fluorescence compared to 0.1 μM. These results were used as a baseline to measure intermolecular protein binding between GFP_{1-10} and FP_{11}. At K_D, split GFP on the rigid scaffold **3** had a ∼ 56% weaker fluorescence than their nonligated counterpart (Figure 1a; **6**). We hypothesize that at concentrations at or higher than K_D, the fluorescence of scaffolded proteins largely originates from intermolecular interactions (e.g., dimerization between scaffolds; Figure 1a, **7**; Scheme S2). However, at 0.1 μM, the nonligated units (**6**) exhibited 30% reduced fluorescence compared to the proteins on the rigid scaffold (**3**). Since this is below K_D, we propose that the observed fluorescence in the scaffolded proteins arises from intramolecular interactions (**5**). TMSD on **3** at 0.1 μM demonstrates that DNA scaffold rigidity inhibits intramolecular PCB. When displaced with strand B′, the resulting flexible DNA scaffold (**5**) had a fluorescence increase, indicating a greater extent of PCB (Figure 1b). Therefore, all subsequent analyses were conducted at 0.1 μM to minimize undesired intermolecular interactions.

The extent of PCB was temporally controlled by introducing the displacement strand B′ (Figure 1c). When strand B was added after displacement to restore the scaffold rigidity (**8**), the fluorescence did not significantly change. Therefore, the DNA interactions that restore the scaffold rigidity did not induce GFP_{1-10} and FP_{11} dissociation. Our observations align with previous reports which posit that noncovalent interactions between GFP_{1-10} and FP_{11} result in observed irreversible binding.[55,59,62] Thus, the DNA interactions used in this work could not override binding between GFP_{1-10} and FP_{11}.

We investigated the impact of scaffold length on the extent of PCB with other scaffolded protein−DNA constructs of different sizes; DNA scaffolds containing 36, 40, 45, and 58 base pairs were synthesized. The 40-base pair scaffold was initially synthesized based on previously reported sequences,[63] while the other scaffolds were designed to ensure antiparallel protein alignment across the helical DNA scaffold. The effect of scaffold length on PCB was studied by comparing the fluorescence of the rigid and flexible forms. Importantly, with the rigid scaffold, between 38 and 58 bp, the extent of PCB increased monotonically. Longer scaffolds are more flexible and therefore allow for more binding events, whereas shorter scaffolds are more rigid and prevent binding between the scaffolded protein fragments, although the increases are less pronounced above 45 bp. In addition, as scaffold length increased, the differences in GFP fluorescence between the flexible and rigid scaffolds became more pronounced, suggesting that scaffold flexibility has a greater effect on PCB (Figure 2a). However, when we synthesized a 78mer scaffold as an upper extreme length to study, there were small differences in fluorescence intensity, suggesting that there is a critical length at which protein binding is independent of scaffold length and behaves as if each complement were free in solution (Figure S10).

We hypothesized that controlling the extent of PCB could confer fine control over protein architecture formation.[64,65] Adjusting the strand length and rigidity should stabilize otherwise unfavorable PCB configurations. Thus, a 58-base pair scaffold and DNA complements of varying lengths were constructed to investigate any resulting effects from scaffold rigidity. We chose to use the longest scaffold investigated here as it should allow for the greatest range of scaffold rigidity (denoted as percent duplexed) and fluorescence. The rigid 58-mer scaffold was produced as previously described and incubated with strand B′ for 1 h to allow for TMSD. Afterward, variants of strand B consisting of 25, 30, 35, 40, 45, or 58 bases (i.e., 43%, 52%, 60%, 69%, 78%, and 100% scaffold duplexed, respectively) were added to the flexible scaffolded proteins.

From Figure 2b, we observed that GFP fluorescence was inversely proportional to strand B length. The largest

https://doi.org/10.1021/jacs.4c11315
J. Am. Chem. Soc. 2024, 146, 32912−32918

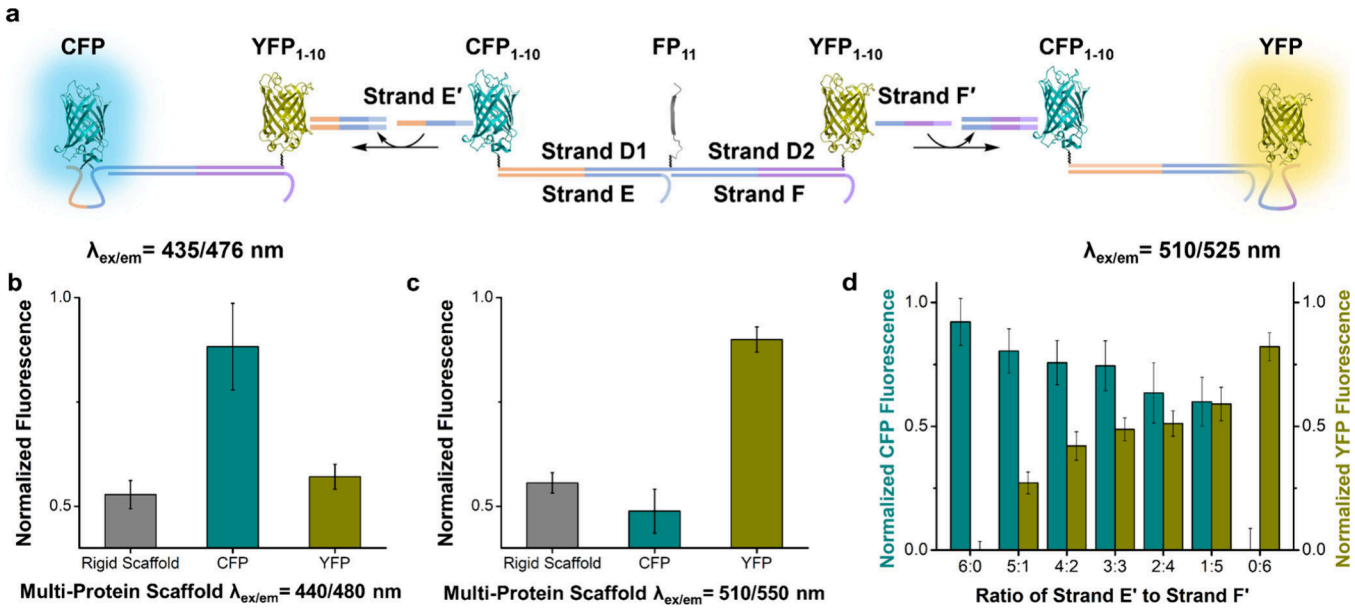

Figure 3. (a) PCB in a multi-protein architecture of CFP_{1-10}, FP_{11}, and YFP_{1-10} is controlled by changing scaffold rigidity in target locations. (b) CFP_{1-10} and FP_{11} bind after strand D1 is made flexible after addition of strand E′, which results in CFP fluorescence ($\lambda_{ex}/\lambda_{em}$ = 440/480 nm, cyan bars). (c) YFP_{1-10} and FP_{11} bind after strand D2 is made flexible after addition of strand F′, which results in YFP fluorescence ($\lambda_{ex}/\lambda_{em}$ = 510/550 nm, yellow bars). (d) Displacement strand stoichiometry (E′:F′) regulates the competitive binding ratio between CFP and YFP.

fluorescence difference was observed between scaffolds with 30- and 25-mer complements (52% and 43% duplexed, respectively). We attribute this trend to the competing effects of DNA duplexation and GFP_{1-10} and FP_{11} complementation: below a characteristic DNA length, GFP_{1-10} and FP_{11} binding overrides any thermodynamic stability conferred by the rigid DNA duplex. Furthermore, there was a 7.5-fold fluorescence increase when scaffolds of higher rigidity were converted to flexible ones (78% and 0% duplexed, respectively). From these results, we postulate that the percentage of scaffold duplexed directly affects its rigidity and thus, the scaffolded PCB.

The sequence specificity of a DNA scaffold should enable orthogonal control over DNA duplexation and, in turn, possibilities for selective and programmable PCB. To test this hypothesis, we independently varied each side of a ternary protein scaffold's rigidity to modulate binding events between unique protein sets (Figures 3a and S11). The UV−vis excitation/emission spectra for the assembled split fluorescent proteins CFP_{1-10}-FP_{11} and YFP_{1-10}-FP_{11} were obtained to orthogonally measure protein fragment binding events (Figure S12). Each protein fragment-DNA construct was then assembled and ligated into a ternary scaffold (Figure 3a and Scheme S3). Next, PCB selectivity was assessed by introducing either strands E′ or F′ to promote binding between FP_{11} and CFP_{1-10} to form CFP, or FP_{11} and YFP_{1-10} to form YFP. Over time, CFP and YFP on the fully rigid scaffold both slightly increased in fluorescence intensity (Figures S13, S14). With the onset of TMSD on strand E, an increase in CFP fluorescence was observed, but not for YFP, which indicates selective control over their binding (Figures 3b and S13). Similarly, TMSD was performed on strand F, which resulted in a selective increase in YFP fluorescence (Figures 3c and S14). From these results, we conclude that sequence-specific DNA interactions enable orthogonal control over different PCB sets within a multi-protein construct.

Finally, it was hypothesized that the extent of strand displacement using different stoichiometries of strand E′ and F′ (incrementing from 0:6 to 6:0) would yield different CFP to YFP ratios. After overnight incubation with the respective combinations of strands, CFP fluorescence intensity concurrently decreased with the strand E′ to F′ ratio (Figure 3d). On the other hand, the YFP fluorescence intensity increased. We hypothesize that differences in the binding affinities between CFP_{1-10}, FP_{11}, and YFP_{1-10} shift the competitive binding equilibrium toward proteins tethered to the more flexible regions. Together, these results suggest that increasing the ratios of target DNA strands can selectively enhance the competitive binding of corresponding target proteins within these multi-protein assemblies. Such control could tune the efficiency of specific protein−protein interactions within higher order protein architectures, thereby allowing for self-regulating mechanisms within these complexes.

This work establishes foundational design parameters to modulate protein binding, notably that the extent of PCB can be increased by either decreasing the rigidity or increasing the length of the scaffold. As such, these parameters offer different handles to regulate the extent of PCB while the DNA sequence specificity controls binding between unique protein sets. To the best of our knowledge, this work is the first demonstration of such control in a multi-protein architecture. While previous DNA nanostructures have been employed to regulate binary PCBs, we have shown how DNA can be used to multiplex these interactions. This proof-of-concept may enable the preparation of nanoscale protein architectures with programmable multi-output functions. Although the synthetic limitations of improving protein−DNA conjugation and ligation yields will need to be addressed for larger scale applications (e.g., DNA origami scaffolds), this system can be extended to incorporate and independently control increasing numbers of different proteins by expanding on the sequence design.[63] This ability sets the stage for synthesizing man-made biological machinery analogous to ATP synthase or motor proteins that require targeted control over unique protein−protein interactions within these multi-protein complexes.[66,67]

https://doi.org/10.1021/jacs.4c11315
J. Am. Chem. Soc. 2024, 146, 32912−32918

■ ASSOCIATED CONTENT

Supporting Information

The Supporting Information is available free of charge at https://pubs.acs.org/doi/10.1021/jacs.4c11315.

DNA sequences, experimental details, characterization, and analytical details including Tables S1−S3 and Figures S1−S18 (PDF)

■ AUTHOR INFORMATION

Corresponding Author

Chad A. Mirkin − *Department of Chemistry, Northwestern University, Evanston, Illinois 60208, United States; Department of Materials Science and Engineering, Department of Chemical and Biological Engineering, Interdisciplinary Biological Sciences Graduate Program, and International Institute for Nanotechnology, Northwestern University, Evanston, Illinois 60208, United States;* orcid.org/0000-0002-6634-7627; Email: chadnano@northwestern.edu

Authors

Yinglun Ma − *Department of Chemistry, Northwestern University, Evanston, Illinois 60208, United States; International Institute for Nanotechnology, Northwestern University, Evanston, Illinois 60208, United States;* orcid.org/0000-0002-1788-0353

Peter H. Winegar − *Department of Chemistry, Northwestern University, Evanston, Illinois 60208, United States; International Institute for Nanotechnology, Northwestern University, Evanston, Illinois 60208, United States;* orcid.org/0000-0003-0984-4990

C. Adrian Figg − *Department of Chemistry, Northwestern University, Evanston, Illinois 60208, United States; International Institute for Nanotechnology, Northwestern University, Evanston, Illinois 60208, United States;* orcid.org/0000-0003-3514-7750

Namrata Ramani − *Department of Materials Science and Engineering and International Institute for Nanotechnology, Northwestern University, Evanston, Illinois 60208, United States;* orcid.org/0000-0001-8159-2842

Alex J. Anderson − *Department of Chemistry, Northwestern University, Evanston, Illinois 60208, United States; International Institute for Nanotechnology, Northwestern University, Evanston, Illinois 60208, United States;* orcid.org/0000-0002-1041-5870

Kathleen Ngo − *Department of Chemistry, Northwestern University, Evanston, Illinois 60208, United States; International Institute for Nanotechnology, Northwestern University, Evanston, Illinois 60208, United States;* orcid.org/0009-0000-0626-1509

John F. Ahrens − *Department of Chemical and Biological Engineering and International Institute for Nanotechnology, Northwestern University, Evanston, Illinois 60208, United States;* orcid.org/0000-0002-1251-1153

Nikhil S. Chellam − *Department of Chemical and Biological Engineering and International Institute for Nanotechnology, Northwestern University, Evanston, Illinois 60208, United States;* orcid.org/0000-0002-8797-876X

Young Jun Kim − *Interdisciplinary Biological Sciences Graduate Program and International Institute for Nanotechnology, Northwestern University, Evanston, Illinois 60208, United States;* orcid.org/0000-0002-5125-3433

Complete contact information is available at: https://pubs.acs.org/10.1021/jacs.4c11315

Notes

The authors declare no competing financial interest.

■ ACKNOWLEDGMENTS

This material is based upon work supported by the National Science Foundation under grants DMR-2104353, DMR-2428112, and DBI-2032180; the Sherman Fairchild Foundation, Inc.; and the Lefkofsky Family Foundation. This research was also supported by the National Cancer Institute of the National Institutes of Health under awards R01CA257926 and R01CA275430. The content is solely the responsibility of the authors and does not necessarily represent the official views of the National Institutes of Health. N.S.C. was supported by the National Science Foundation through the National Science Foundation Graduate Research Fellowship Program under grant DGE-2234667. Any opinions, findings, and conclusions or recommendations expressed in this material are those of the author(s) and do not necessarily reflect the views of the National Science Foundation. This work made use of the IMSERC MS facility at Northwestern University, which has received support from the Soft and Hybrid Nanotechnology Experimental (SHyNE) Resource (NSF ECCS-2025633), the State of Illinois, and the International Institute for Nanotechnology (IIN). The authors thank Cuizheng Zhang and Tanushri Sengupta (Northwestern University) for scientific discussions and editorial input. Molecular graphics and analyses were performed with UCSF Chimera, developed by the Resource for Biocomputing, Visualization, and Informatics at the University of California, San Francisco, with support from NIH P41-GM103311.

■ REFERENCES

(1) Reichmann, D.; Rahat, O.; Cohen, M.; Neuvirth, H.; Schreiber, G. The molecular architecture of protein−protein binding sites. *Curr. Opin. Struct. Biol.* **2007**, *17* (1), 67−76.

(2) Ahnert, S. E.; Marsh, J. A.; Hernández, H.; Robinson, C. V.; Teichmann, S. A. Principles of assembly reveal a periodic table of protein complexes. *Science* **2015**, *350* (6266), No. aaa2245.

(3) Luo, Q.; Hou, C.; Bai, Y.; Wang, R.; Liu, J. Protein Assembly: Versatile Approaches to Construct Highly Ordered Nanostructures. *Chem. Rev.* **2016**, *116* (22), 13571−13632.

(4) Pieters, B. J. G. E.; Van Eldijk, M. B.; Nolte, R. J. M.; Mecinović, J. Natural supramolecular protein assemblies. *Chem. Soc. Rev.* **2016**, *45* (1), 24−39.

(5) Zhu, J.; Avakyan, N.; Kakkis, A.; Hoffnagle, A. M.; Han, K.; Li, Y.; Zhang, Z.; Choi, T. S.; Na, Y.; Yu, C.-J.; et al. Protein assembly by design. *Chem. Rev.* **2021**, *121* (22), 13701−13796.

(6) Li, Y.; Tian, R.; Shi, H.; Xu, J.; Wang, T.; Liu, J. Protein assembly: Controllable design strategies and applications in biology. *Aggreg.* **2023**, *4* (3), No. e317.

(7) Bale, J. B.; Gonen, S.; Liu, Y.; Sheffler, W.; Ellis, D.; Thomas, C.; Cascio, D.; Yeates, T. O.; Gonen, T.; King, N. P.; et al. Accurate design of megadalton-scale two-component icosahedral protein complexes. *Science* **2016**, *353* (6297), 389−394.

(8) Praetorius, F.; Leung, P. J. Y.; Tessmer, M. H.; Broerman, A.; Demakis, C.; Dishman, A. F.; Pillai, A.; Idris, A.; Juergens, D.; Dauparas, J.; et al. Design of stimulus-responsive two-state hinge proteins. *Science* **2023**, *381* (6659), 754−760.

(9) Rennella, E.; Sahtoe, D. D.; Baker, D.; Kay, L. E. Exploiting conformational dynamics to modulate the function of designed proteins. *Proc. Natl. Acad. Sci. U.S.A.* **2023**, *120* (18), No. e2303149120.

(10) Wright, A. V.; Sternberg, S. H.; Taylor, D. W.; Staahl, B. T.; Bardales, J. A.; Kornfeld, J. E.; Doudna, J. A. Rational design of a split-Cas9 enzyme complex. *Proc. Natl. Acad. Sci. U.S.A.* **2015**, *112* (10), 2984−2989.
(11) Koh, M.; Nasertorabi, F.; Han, G. W.; Stevens, R. C.; Schultz, P. G. Generation of an Orthogonal Protein−Protein Interface with a Noncanonical Amino Acid. *J. Am. Chem. Soc.* **2017**, *139* (16), 5728−5731.
(12) Mogilevsky, C. S.; Lobba, M. J.; Brauer, D. D.; Marmelstein, A. M.; Maza, J. C.; Gleason, J. M.; Doudna, J. A.; Francis, M. B. Synthesis of Multi-Protein Complexes through Charge-Directed Sequential Activation of Tyrosine Residues. *J. Am. Chem. Soc.* **2021**, *143* (34), 13538−13547.
(13) Mumby, E. J.; Willoughby, J. A.; Vasquez, C.; Delavari, N.; Zhang, Z.; Clark, C. T.; Stull, F. Binding Interface and Electron Transfer Between Nicotine Oxidoreductase and Its Cytochrome c Electron Acceptor. *Biochemistry* **2022**, *61* (20), 2182−2187.
(14) Zubi, Y. S.; Seki, K.; Li, Y.; Hunt, A. C.; Liu, B.; Roux, B.; Jewett, M. C.; Lewis, J. C. Metal-responsive regulation of enzyme catalysis using genetically encoded chemical switches. *Nat. Commun.* **2022**, *13* (1), 1864.
(15) Callahan, B. P.; Stanger, M. J.; Belfort, M. Protease Activation of Split Green Fluorescent Protein. *ChemBioChem.* **2010**, *11* (16), 2259−2263.
(16) Lai, Y.-T.; King, N. P.; Yeates, T. O. Principles for designing ordered protein assemblies. *Trends Cell Biol.* **2012**, *22* (12), 653−661.
(17) Arkin, M. R.; Tang, Y.; Wells, J. A. Small-molecule inhibitors of protein-protein interactions: progressing toward the reality. *Chem. Biol.* **2014**, *21* (9), 1102−1114.
(18) Wang, H.; Vilela, M.; Winkler, A.; Tarnawski, M.; Schlichting, I.; Yumerefendi, H.; Kuhlman, B.; Liu, R.; Danuser, G.; Hahn, K. M. LOVTRAP: an optogenetic system for photoinduced protein dissociation. *Nat. Methods* **2016**, *13* (9), 755−758.
(19) Bobrovnikov, D.; Makurath, M. A.; Wolfe, C. H.; Chemla, Y. R.; Ha, T. Helicase Activity Modulation with On-Demand Light-Based Conformational Control. *J. Am. Chem. Soc.* **2023**, *145* (39), 21253−21262.
(20) Listov, D.; Goverde, C. A.; Correia, B. E.; Fleishman, S. J. Opportunities and challenges in design and optimization of protein function. *Nat. Rev. Mol. Cell Biol.* **2024**, *25*, 639−653.
(21) Kim, Y. E.; Kim, Y.-N.; Kim, J. A.; Kim, H. M.; Jung, Y. Green fluorescent protein nanopolygons as monodisperse supramolecular assemblies of functional proteins with defined valency. *Nat. Commun.* **2015**, *6* (1), 7134.
(22) Bhaskar, S.; Lim, S. Engineering protein nanocages as carriers for biomedical applications. *NPG Asia Mater.* **2017**, *9* (4), e371−e371.
(23) Mirkin, C. A.; Letsinger, R. L.; Mucic, R. C.; Storhoff, J. J. A DNA-based method for rationally assembling nanoparticles into macroscopic materials. *Nature* **1996**, *382* (6592), 607−609.
(24) Douglas, S. M.; Bachelet, I.; Church, G. M. A Logic-Gated Nanorobot for Targeted Transport of Molecular Payloads. *Science* **2012**, *335* (6070), 831−834.
(25) Wilner, O. I.; Willner, I. Functionalized DNA Nanostructures. *Chem. Rev.* **2012**, *112* (4), 2528−2556.
(26) Yang, Y. R.; Liu, Y.; Yan, H. DNA Nanostructures as Programmable Biomolecular Scaffolds. *Bioconjugate Chem.* **2015**, *26* (8), 1381−1395.
(27) Wagenbauer, K. F.; Sigl, C.; Dietz, H. Gigadalton-scale shape-programmable DNA assemblies. *Nature* **2017**, *552* (7683), 78−83.
(28) Laramy, C. R.; O'Brien, M. N.; Mirkin, C. A. Crystal engineering with DNA. *Nat. Rev. Mater.* **2019**, *4* (3), 201−224.
(29) McMillan, J. R.; Hayes, O. G.; Winegar, P. H.; Mirkin, C. A. Protein Materials Engineering with DNA. *Acc. Chem. Res.* **2019**, *52* (7), 1939−1948.
(30) Woloszyn, K.; Vecchioni, S.; Ohayon, Y. P.; Lu, B.; Ma, Y.; Huang, Q.; Zhu, E.; Chernovolenko, D.; Markus, T.; Jonoska, N.; et al. Augmented DNA Nanoarchitectures: A Structural Library of 3D Self-Assembling Tensegrity Triangle Variants. *Adv. Mater.* **2022**, *34* (49), No. 2206876.
(31) Zhang, C.; Zhao, J.; Lu, B.; Seeman, N. C.; Sha, R.; Noinaj, N.; Mao, C. Engineering DNA Crystals toward Studying DNA−Guest Molecule Interactions. *J. Am. Chem. Soc.* **2023**, *145* (8), 4853−4859.
(32) Brodin, J. D.; Auyeung, E.; Mirkin, C. A. DNA-mediated engineering of multicomponent enzyme crystals. *Proc. Natl. Acad. Sci. U.S.A.* **2015**, *112* (15), 4564−4569.
(33) Xiang, B.; He, K.; Zhu, R.; Liu, Z.; Zeng, S.; Huang, Y.; Nie, Z.; Yao, S. Self-Assembled DNA Hydrogel Based on Enzymatically Polymerized DNA for Protein Encapsulation and Enzyme/DNAzyme Hybrid Cascade Reaction. *ACS Appl. Mater. Interfaces* **2016**, *8* (35), 22801−22807.
(34) Mcmillan, J. R.; Brodin, J. D.; Millan, J. A.; Lee, B.; Olvera De La Cruz, M.; Mirkin, C. A. Modulating Nanoparticle Superlattice Structure Using Proteins with Tunable Bond Distributions. *J. Am. Chem. Soc.* **2017**, *139* (5), 1754−1757.
(35) Hayes, O. G.; Mcmillan, J. R.; Lee, B.; Mirkin, C. A. DNA-Encoded Protein Janus Nanoparticles. *J. Am. Chem. Soc.* **2018**, *140* (29), 9269−9274.
(36) Mcmillan, J. R.; Mirkin, C. A. DNA-Functionalized, Bivalent Proteins. *J. Am. Chem. Soc.* **2018**, *140* (22), 6776−6779.
(37) McMillan, J. R.; Hayes, O. G.; Remis, J. P.; Mirkin, C. A. Programming Protein Polymerization with DNA. *J. Am. Chem. Soc.* **2018**, *140* (46), 15950−15956.
(38) Winegar, P. H.; Hayes, O. G.; McMillan, J. R.; Figg, C. A.; Focia, P. J.; Mirkin, C. A. DNA-Directed Protein Packing within Single Crystals. *Chem.* **2020**, *6* (4), 1007−1017.
(39) Hayes, O. G.; Partridge, B. E.; Mirkin, C. A. Encoding hierarchical assembly pathways of proteins with DNA. *Proc. Natl. Acad. Sci. U.S.A.* **2021**, *118* (40), No. e2106808118.
(40) Partridge, B. E.; Winegar, P. H.; Han, Z.; Mirkin, C. A. Redefining Protein Interfaces within Protein Single Crystals with DNA. *J. Am. Chem. Soc.* **2021**, *143* (23), 8925−8934.
(41) Cissell, K. A.; Rahimi, Y.; Shrestha, S.; Deo, S. K. Reassembly of a Bioluminescent Protein Renilla Luciferase Directed through DNA Hybridization. *Bioconjugate Chem.* **2009**, *20* (1), 15−19.
(42) Janssen, B. M. G.; Engelen, W.; Merkx, M. DNA-Directed Control of Enzyme−Inhibitor Complex Formation: A Modular Approach to Reversibly Switch Enzyme Activity. *ACS Synth. Biol.* **2015**, *4* (5), 547−553.
(43) Janssen, B. M. G.; van Rosmalen, M.; van Beek, L.; Merkx, M. Antibody Activation using DNA-Based Logic Gates. *Angew. Chem., Int. Ed. Engl.* **2015**, *54* (8), 2530−2533.
(44) Engelen, W.; Janssen, B. M. G.; Merkx, M. DNA-based control of protein activity. *Chem. Commun.* **2016**, *52* (18), 3598−3610.
(45) Zhang, Y.; Pan, V.; Li, X.; Yang, X.; Li, H.; Wang, P.; Ke, Y. Dynamic DNA Structures. *Small* **2019**, *15* (26), No. 1900228.
(46) Snider, D. M.; Pandit, S.; Coffin, M. L.; Ebrahimi, S. B.; Samanta, D. DNA-Mediated Control of Protein Function in Semi-Synthetic Systems. *ChemBioChem.* **2022**, *23* (24), No. e202200464.
(47) Choi, B.; Zocchi, G.; Wu, Y.; Chan, S.; Jeanne Perry, L. Allosteric Control through Mechanical Tension. *Phys. Rev. Lett.* **2005**, *95* (7), No. 078102.
(48) Demidov, V. V.; Dokholyan, N. V.; Witte-Hoffmann, C.; Chalasani, P.; Yiu, H.-W.; Ding, F.; Yu, Y.; Cantor, C. R.; Broude, N. E. Fast complementation of split fluorescent protein triggered by DNA hybridization. *Proc. Natl. Acad. Sci. U.S.A.* **2006**, *103* (7), 2052−2056.
(49) Oltra, S. N.; Bos, J.; Roelfes, G. Control over Enzymatic Activity by DNA-Directed Split Enzyme Reassembly. *ChemBioChem.* **2010**, *11* (16), 2255−2258.
(50) Fu, J.; Liu, M.; Liu, Y.; Woodbury, N. W.; Yan, H. Interenzyme Substrate Diffusion for an Enzyme Cascade Organized on Spatially Addressable DNA Nanostructures. *J. Am. Chem. Soc.* **2012**, *134* (12), 5516−5519.
(51) Fu, J.; Yang, Y. R.; Johnson-Buck, A.; Liu, M.; Liu, Y.; Walter, N. G.; Woodbury, N. W.; Yan, H. Multi-enzyme complexes on DNA

https://doi.org/10.1021/jacs.4c11315
J. Am. Chem. Soc. 2024, 146, 32912−32918

scaffolds capable of substrate channelling with an artificial swinging arm. *Nat. Nanotechnol.* **2014**, *9* (7), 531−536.
(52) Linko, V.; Eerikäinen, M.; Kostiainen, M. A. A modular DNA origami-based enzyme cascade nanoreactor. *Chem. Commun.* **2015**, *51* (25), 5351−5354.
(53) Chen, R. P.; Blackstock, D.; Sun, Q.; Chen, W. Dynamic protein assembly by programmable DNA strand displacement. *Nat. Chem.* **2018**, *10* (4), 474−481.
(54) Cabantous, S.; Terwilliger, T. C.; Waldo, G. S. Protein tagging and detection with engineered self-assembling fragments of green fluorescent protein. *Nat. Biotechnol.* **2005**, *23* (1), 102−107.
(55) Romei, M. G.; Boxer, S. G. Split Green Fluorescent Proteins: Scope, Limitations, and Outlook. *Annu. Rev. Biophys.* **2019**, *48*, 19−44.
(56) Kamiyama, D.; Sekine, S.; Barsi-Rhyne, B.; Hu, J.; Chen, B.; Gilbert, L. A.; Ishikawa, H.; Leonetti, M. D.; Marshall, W. F.; Weissman, J. S.; et al. Versatile protein tagging in cells with split fluorescent protein. *Nat. Commun.* **2016**, *7* (1), No. 11046.
(57) Huang, Y.-M.; Bystroff, C. Complementation and Reconstitution of Fluorescence from Circularly Permuted and Truncated Green Fluorescent Protein. *Biochemistry* **2009**, *48* (5), 929−940.
(58) Deng, A.; Boxer, S. G. Structural Insight into the Photochemistry of Split Green Fluorescent Proteins: A Unique Role for a His-Tag. *J. Am. Chem. Soc.* **2018**, *140* (1), 375−381.
(59) Köker, T.; Fernandez, A.; Pinaud, F. Characterization of Split Fluorescent Protein Variants and Quantitative Analyses of Their Self-Assembly Process. *Sci. Rep.* **2018**, *8* (1), 5344.
(60) Lin, C.-Y.; Romei, M. G.; Oltrogge, L. M.; Mathews, I. I.; Boxer, S. G. Unified Model for Photophysical and Electro-Optical Properties of Green Fluorescent Proteins. *J. Am. Chem. Soc.* **2019**, *141* (38), 15250−15265.
(61) Xin, L.; Zhou, C.; Yang, Z.; Liu, D. Regulation of an Enzyme Cascade Reaction by a DNA Machine. *Small* **2013**, *9* (18), 3088−3091.
(62) Cabantous, S.; Nguyen, H. B.; Pedelacq, J.-D.; Koraïchi, F.; Chaudhary, A.; Ganguly, K.; Lockard, M. A.; Favre, G.; Terwilliger, T. C.; Waldo, G. S. A New Protein-Protein Interaction Sensor Based on Tripartite Split-GFP Association. *Sci. Rep.* **2013**, *3* (1), 2854.
(63) Winegar, P. H.; Figg, C. A.; Teplensky, M. H.; Ramani, N.; Mirkin, C. A. Modular nucleic acid scaffolds for synthesizing monodisperse and sequence-encoded antibody oligomers. *Chem.* **2022**, *8* (11), 3018−3030.
(64) Liu, M.; Fu, J.; Hejesen, C.; Yang, Y.; Woodbury, N. W.; Gothelf, K.; Liu, Y.; Yan, H. A DNA tweezer-actuated enzyme nanoreactor. *Nat. Commun.* **2013**, *4* (1), 2127.
(65) Rosier, B. J. H. M.; Markvoort, A. J.; Gumí Audenis, B.; Roodhuizen, J. A. L.; Den Hamer, A.; Brunsveld, L.; De Greef, T. F. A. Proximity-induced caspase-9 activation on a DNA origami-based synthetic apoptosome. *Nat. Catal.* **2020**, *3* (3), 295−306.
(66) Sweeney, H. L.; Holzbaur, E. L. F. Motor Proteins. *Cold Spring Harb. Perspect. Biol.* **2018**, *10* (5), No. a021931.
(67) Nirody, J. A.; Budin, I.; Rangamani, P. ATP synthase: Evolution, energetics, and membrane interactions. *J. Gen. Physiol.* **2020**, *152* (11), No. e201912475.

https://doi.org/10.1021/jacs.4c11315
J. Am. Chem. Soc. 2024, 146, 32912−32918